doi:10.1093/brain/awp078 Brain 2009: 132; 1711–1722 | 1711

BRAIN
A JOURNAL OF NEUROLOGY

Early- and late-onset inherited erythromelalgia: genotype–phenotype correlation

Chongyang Han,[1,2] Sulayman D. Dib-Hajj,[1,2] Zhimiao Lin,[3] Yan Li,[3] Emmanuella M. Eastman,[1,2] Lynda Tyrrell,[1,2] Xianwei Cao,[4] Yong Yang[3,*] and Stephen G. Waxman[1,2,*]

1 Department of Neurology and Center for Neuroscience and Regeneration Research, Yale University School of Medicine, New Haven, CT 06510, USA
2 Rehabilitation Research Center, Veterans Affairs Connecticut Healthcare System, West Haven, CT 06516, USA
3 Department of Dermatology, Peking University First Hospital, Beijing 100034, China
4 Department of Dermatology, First Affiliated Hospital of Nanchang University, Nanchang, Jiangxi 33006, China

*These authors contributed equally to this work.

Correspondence to: Stephen G. Waxman, MD, PhD,
Department of Neurology,
LCI 707, Yale University School of Medicine,
333 Cedar Street,
New Haven,
CT 06520-8018, USA
E-mail: Stephen.Waxman@yale.edu

Correspondence may also be addressed to: Yong Yang, MD, PhD
Department of Dermatology,
Peking University First Hospital,
No 8 Xishiku Street, Xicheng District,
Beijing 100034, China
E-mail: dryongyang@bjmu.edu.cn

Inherited erythromelalgia (IEM), an autosomal dominant disorder characterized by severe burning pain in response to mild warmth, has been shown to be caused by gain-of-function mutations of sodium channel $Na_v1.7$ which is preferentially expressed within dorsal root ganglion (DRG) and sympathetic ganglion neurons. Almost all physiologically characterized cases of IEM have been associated with onset in early childhood. Here, we report the voltage-clamp and current-clamp analysis of a new $Na_v1.7$ mutation, Q10R, in a patient with clinical onset of erythromelalgia in the second decade. We show that the mutation in this patient hyperpolarizes activation by only −5.3 mV, a smaller shift than seen with early-onset erythromelalgia mutations, but similar to that of I136V, another mutation that is linked to delayed-onset IEM. Using current-clamp, we show that the expression of Q10R induces hyperexcitability in DRG neurons, but produces an increase in excitability that is smaller than the change produced by I848T, an early-onset erythromelalgia mutation. Our analysis suggests a genotype–phenotype relationship at three levels (clinical, cellular and molecular/ion channel), with mutations that produce smaller effects on sodium channel activation being associated with a smaller degree of DRG neuron excitability and later onset of clinical signs.

Keywords: channelopathy; erythromelalgia; pain; sodium channel

Abbreviations: AL = adult-long; DRG = dorsal root ganglion; HEK 293 = human embryonic kidney cells; IEM = Inherited erythromelalgia; NS = neonatal-short; WT = wild-type

Received January 9, 2009. Revised February 20, 2009. Accepted February 23, 2009. Advance Access publication April 15, 2009

Introduction

Inherited erythromelalgia (IEM, also termed erythermalgia), an autosomal dominant disorder characterized by severe burning pain and erythema of the extremities triggered by warmth, has been linked to gain-of-function mutations in *SCN9A*, the gene encoding $Na_v1.7$ (Dib-Hajj *et al*., 2007; Drenth and Waxman, 2007), a voltage-gated sodium channel that is preferentially expressed in dorsal root ganglion (DRG) neurons, particularly nociceptors, and sympathetic ganglion neurons (Black *et al*., 1996; Sangameswaran *et al*., 1997; Toledo-Aral *et al*., 1997; Djouhri *et al*., 2003). $Na_v1.7$ produces rapidly activating and inactivating tetrodotoxin-sensitive currents that recover slowly from fast-inactivation (Cummins *et al*., 1998). As a result of its slow closed-state inactivation, $Na_v1.7$ is able to respond to slow, small depolarizations close to resting membrane potential, thus amplifying sub-threshold stimuli (Cummins *et al*., 1998) so as to set the gain on nociceptors (Waxman, 2006). Gain-of-function mutations of $Na_v1.7$ might thus be expected to contribute to nociceptor hyperexcitability, thereby producing pain in patients with erythromelalgia.

Thus far, nine mutations of $Na_v1.7$ linked to IEM have been characterized by electrophysiological analysis (Cummins *et al*., 2004; Dib-Hajj *et al*., 2005; Choi *et al*., 2006; Han *et al*., 2006; Harty *et al*., 2006; Lampert *et al*., 2006; Sheets *et al*., 2007; Cheng *et al*., 2008). Erythromelalgia mutations studied to date produce a hyperpolarizing shift in activation, slow deactivation and in most cases enhance the response in $Na_v1.7$ channels to slow ramp-like stimuli. Each of these changes has been predicted to increase the excitability of DRG neurons in which $Na_v1.7$ mutant channels are expressed, with computer simulations suggesting that the shift in activation has the largest effect (Sheets *et al*., 2007).

Of the erythromelalgia mutations that have been characterized electrophysiologically thus far, almost all have been linked to families with onset in early childhood (infancy to 6 years of age) (Cummins *et al*., 2004; Dib-Hajj *et al*., 2005; Choi *et al*., 2006; Han *et al*., 2006; Harty *et al*., 2006; Lampert *et al*., 2006; Sheets *et al*., 2007). A single mutation, I136V, linked to a family with later age of onset, with pain appearing first in the feet in the second decade of life (Lee *et al*., 2007), has been characterized electrophysiologically by voltage-clamp (Cheng *et al*., 2008), and has been shown to alter the function of $Na_v1.7$ channels via a shifting of the voltage-dependence of activation by −5.7 mV, a smaller shift than for other IEM mutations that have been characterized (−7.6 to −13.8 mV). Here, we report a new mutation in $Na_v1.7$, Q10R, from a patient with erythromelalgia with onset during the second decade of life, and examine its effect on function at the cellular (DRG neuron firing pattern) as well as ion channel ($Na_v1.7$) level. Using voltage-clamp methods, we show that this mutation slows deactivation and hyperpolarizes the voltage-dependence of activation of the $Na_v1.7$ channel, but to a smaller degree than mutations linked to early-onset erythromelalgia. We also show that splice variant switching does not result in a larger effect of the Q10R mutation in adult isoforms of $Na_v1.7$. To study the effect of the Q10R mutation on firing of DRG neurons, we used current-clamp recording, and show that this mutation produces DRG neuron hyperexcitabilty. We also demonstrate, however, that the increase in DRG neuron excitability produced by the Q10R mutation from a patient with relatively late disease onset is less pronounced than the hyperexcitabilty produced by I848T, an early-onset erythromelalgia mutation. Taken together, these results provide evidence for a genotype–phenotype relationship at the clinical, cellular and molecular levels.

Materials and Methods

Patient

A blood sample was obtained at age 17 from the male proband who began to experience excruciating pain, warmth and redness in both feet and lower legs at the age of 14. Family consent was obtained according to the institutional review board protocol and blood samples were then obtained and analysed for mutations in *SCN9A*.

Exon screening

Genomic DNA was extracted from blood samples of all family members. PCR amplification of the 26 exons of *SCN9A* was performed and the amplicons were purified and sequenced as previously described (Yang *et al*., 2004). Genomic sequences were compared to reference $Na_v1.7$ cDNA (Klugbauer *et al*., 1995) to identify sequence variation.

Voltage-clamp analysis

The Q10R mutation was introduced into the neonatal short (NS) splice variant of the tetrodotoxin-resistant version of human $Na_v1.7$ cDNA (Herzog *et al*., 2003) using QuickChange XL site-directed mutagenesis (Stratagene, La Jolla, CA, USA). Human embryonic kidney cells (HEK 293) were transfected with the Q10R/NS mutant channel construct using Satisfaction reagents (Stratagene). Transfected HEK 293 cells, grown under standard culture conditions (5% CO_2, 37°C) in Dulbeccos's modified Eagle's medium supplemented with 10% fetal bovine serum, were treated with G418 for several weeks to derive stable cell lines that express the mutant channel. For comparison, Q10R was introduced into the adult/long ($hNa_v1.7_R$/AL) variant (Raymond *et al*., 2004) by site-directed mutagenesis. $Na_v1.7_R$/AL and Q10R/AL were transiently transfected into HEK 293, and sodium currents were measured 24 h after transfection. The presence of at least four β-subunits within DRG neurons presented a very large number of combinational possibilities that precluded an analysis of β-subunit effects. Unless otherwise noted, all studies were carried out using the NS splice form of $Na_v1.7$.

Whole-cell voltage-clamp recordings of HEK 293 cells expressing either wild-type (WT) $Na_v1.7_R$ or Q10R mutant channels were performed at room temperature (20–22°C) using an EPC-9 amplifier (HEKA Electronics, Lambrecht/Pfalz, Germany). Fire-polished electrodes (0.6–1.5 MΩ) were fabricated from 1.6 mm outer diameter borosilicate glass micropipettes (World Precision Instruments, Sarasota, FL, USA). The pipette potential was adjusted to zero before seal formation, and liquid junction potential was not corrected. Capacity transients were cancelled and voltage errors were minimized with 80–90% series resistance compensation. Currents were acquired with Pulse Software (HEKA Electronics), 5 min after establishing whole-cell configuration, sampled at a rate of 50 kHz, and filtered at 2.9 kHz.

For current–voltage relationships, cells were held at −100 mV and stepped to a range of potentials (−80 to +60 mV in 5 mV increments) for 40 ms. Peak inward currents (I) were plotted as a function of depolarization potential to generate I–V curves. Activation curves were obtained by converting I to conductance (G) at each voltage (V) using the equation $G = I/(V - V_{rev})$, where V_{rev} is the reversal potential which was determined for each cell individually. Activation curves were then fit with Boltzmann functions in the form of $G = G_{max}/\{1 + \exp[(V_{1/2,act} - V)/k]\}$, where G_{max} is the maximal sodium conductance, $V_{1/2,act}$ is the potential at which activation is half-maximal, V is the test potential and k is the slope factor.

Steady-state fast inactivation was achieved with a series of 500-ms prepulses (−150 to 0 mV in 10 mV increments) and the remaining non-inactivated channels were activated by a 40 ms step depolarization to −10 mV. Steady-state slow inactivation was determined with 30 s prepulses ranging from −130 to 10 mV followed by a 100 ms hyperpolarization at −120 mV to remove fast inactivation. Remaining available channels were activated by a 20 ms test pulse to −10 mV. Peak inward currents obtained from steady-state fast inactivation and slow inactivation protocols were normalized to the maximal peak current (I_{max}) and fit with Boltzman functions:

$$I/I_{max} = 1/\{1 + \exp[(V - V_{1/2,\,inact})/k]\}$$

for fast inactivation, and

$$I/I_{max} = R_{in} + (1 - R_{in})/\{1 + \exp[(V - V_{1/2,\,inact})/k]\}$$

for slow inactivation.

where V represents the inactivating prepulse potential, $V_{1/2,inact}$ represents the midpoint of the inactivation curve and R_{in} is the fraction of channels that are resistant to inactivation.

Deactivation was estimated from current decay, using a short (0.5 ms) depolarizing pulse to −20 mV followed by a 100 ms repolarizing pulse to potentials ranging from −100 to −40 mV with 5 mV increments. Deactivation kinetics were calculated by fitting the decaying currents with a single exponential function. Ramp currents were elicited with a slow depolarizing voltage ramp from −100 to 20 mV at a rate of 0.2 mV/ms. The absolute ramp current amplitude was normalized to the maximal peak current obtained by I–V protocol.

The pipette solution contained (in mM): 140 CsF, 10 NaCl, 1 EGTA and 10 HEPES, pH 7.30 (adjusted with CsOH). Osmolarity was adjusted to 310 mOsmol/l with dextrose. The extracellular bath solution contained (in mM): 140 NaCl, 3 KCl, 1 $MgCl_2$, 1 $CaCl_2$, 10 dextrose, 10 HEPES, pH 7.4 (adjusted with NaOH) and the osmolarity was adjusted to 315 mOsmol/l with dextrose. Tetrodotoxin (300 nM) was added to the bath solution to block endogenous voltage-gated sodium currents in HEK293 cells (Cummins *et al*., 1999), permitting currents from WT $Na_v1.7_R$ or Q10R to be recorded in isolation.

Transfection of DRG neurons and current-clamp electrophysiology

The protocol for the care and sacrifice of rats used in the study was approved by the Veterans Administration Connecticut Healthcare system IACUC. DRG tissue from 1- to 5-day old Sprague Dawley rats were harvested and dissociated using a protocol (Dib-Hajj *et al*., 2008) that was adapted from Rizzo *et al*. (1994). Sodium channel and GFP constructs (channel:GFP ratio of 5: 1) were electroporated into DRG neurons using Rat Neuron Nucleofector Solution (Amaxa, Gaithersburg, MD, USA) with WT $Na_V1.7_R$,Q10R, I848T mutant derivative as described previously (Dib-Hajj *et al*., 2005; Harty *et al*., 2006; Rush *et al*., 2006; Dib-Hajj *et al*., 2008). Transfected DRG neurons were incubated at 37°C in Ca^{2+}- and Mg^{2+}- free culture medium (DMEM plus 10% fetal calf serum) for 5 min to increase cell viability. The cell suspension was then diluted in culture medium supplemented with nerve growth factor and glial cell line-derived neurotrophic factor (50 ng/ml), plated on 12 mm circular coverslips coated with laminin and poly-ornithine and incubated at 37°C in 5% CO_2.

Small (<25 μm) GFP-labelled DRG neurons were used for current-clamp recording 18–36 h after transfection. Previous studies have shown that there are no significant differences in resting potential, input resistance, action potential current threshold, action potential amplitude or repetitive firing in small DRG neurons transfected with WT $Na_v1.7_R$ plus GFP, compared with GFP alone (Harty *et al*., 2006). Electrodes had a resistance of 1–3 MΩ when filled with the pipette solution, which contained the following (in mM): 140 KCl, 0.5 EGTA, 5 HEPES and 3 Mg-ATP, pH 7.3 with KOH (adjusted to 315 mOsm with dextrose). The extracellular solution contained the following (in mM): 140 NaCl, 3 KCl, 2 $MgCl_2$, 2 $CaCl_2$, 10 HEPES, pH 7.3 with NaOH (adjusted to 320 mOsm with dextrose). Solution application and signal acquisition were the same as for voltage-clamp recording. Whole-cell configuration was obtained in voltage-clamp mode before proceeding to the current-clamp recording mode. Cells with stable (<10% variation) resting membrane potentials more negative than −40 mV were used for data collection. Threshold was determined by the first action potential elicited by a series of depolarizing current injections that increased in 5 pA increments.

Data analysis

Data were analysed using PulseFit 8.77 (HEKA Electronics) and Origin 8.0 (Microcal Software, Northampton, MA, USA), and presented as means ± SE. Except where noted, statistical significance was determined by unpaired Student's t-tests. For multi-group statistical analysis, we used one-way ANOVA followed by Tukey *post hoc* test or Kruskal–Wallis followed by Dunn procedure depending on the normal distribution of the data.

Results

Clinical description

This male Chinese patient was well until age 14 years when he began to experience excruciating pain, warmth and redness of both feet and lower legs. The pain could be provoked by exposure to warmth and by exercise. The frequency and severity of the pain progressed, and it became almost constant, interfering with walking at the time of evaluation at the age of 17 years. The patient's hands were not affected. The patient did not have siblings, and there was no family history. Blood and urine profiles, hepatic and renal functions were normal. The pain was not responsive to aspirin or mexiletine.

Q10R mutation

Sequence analysis of *SCN9A* coding exons demonstrated an A to G substitution (c.29A > G) in exon 1 in the proband. This single nucleotide mutation causes the substitution of glutamine 10 with arginine (Q10R) in the cytoplasmic N-terminus of the

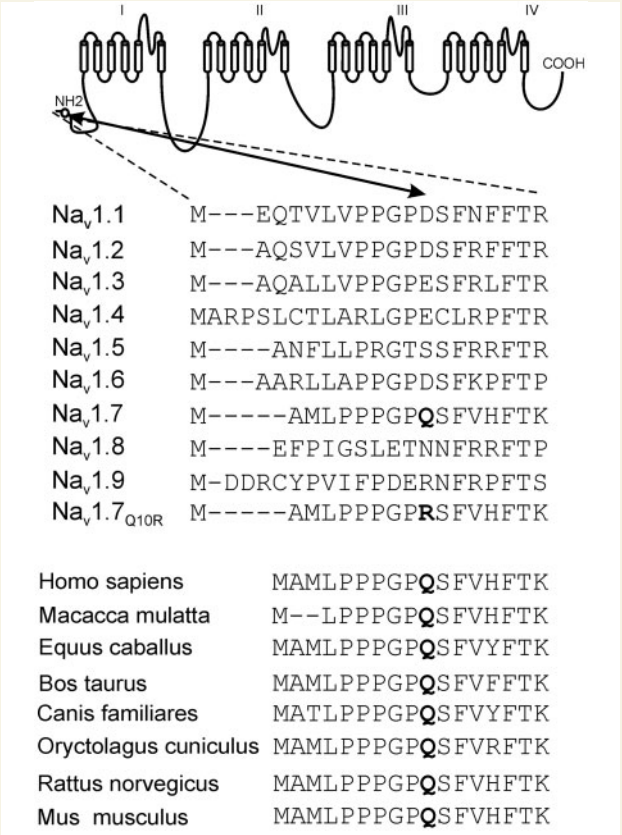

Figure 1 Schematic of a voltage-gated sodium channel α-subunit showing the location of the Q10R (bold) mutation and the aligned N-terminus sequences for the Nav1 subfamily, and Na$_v$1.7 orthologues that have been reported to date in the protein database, showing the conserved Q10 residue (bold).

channel (Fig. 1). While Q10 is not conserved in other members of the sodium channel family, it is conserved in the Na$_v$1.7 orthologues that have been reported to date from different species (Fig. 1). The c.29A>G mutation was absent from both parents, and from 200 alleles from normal Chinese controls, indicating that this mutation is unlikely to be a polymorphism.

Voltage-clamp characterization: hyperpolarized activation and slower deactivation

Figure 2A shows representative Na$_v$1.7 sodium currents recorded using whole-cell patch-clamp from cells expressing WT/NS variant (hNa$_v$1.7/NS) channels (Raymond *et al*., 2004), and Fig. 2B from cells expressing Q10R/NS mutant channels. Peak current densities of the two cell lines were: Na$_v$1.7$_R$ = 423 ± 28 pA/pF (n = 43), and Q10R = 587 ± 29 pA/pF (n = 48). To examine the voltage dependence of activation, cells were held at −100 mV and stepped to a range of potentials (−80 to +60 mV in 5 mV increments) for 40 ms. As shown in Fig. 2C and D, Q10R channels exhibit a hyperpolarized current–voltage and conductance–voltage curve compared to WT channels. When fitted with Boltzmann plots, the midpoint of activation was significantly more negative for Q10R channels (−30.0 ± 0.4 mV, n = 48) than for WT channels (−24.7 ± 0.5 mV, P < 0.001; n = 43), a shift of −5.3 mV in the hyperpolarizing direction.

Kinetics of activation, which reflect the transition from the closed to open state, were investigated by measuring the time-to-peak of the transient current. The rate of activation for Q10R was significantly faster (P < 0.05) than WT at potentials ranging from −40 to +10 mV (Fig. 2E). Kinetics of deactivation, which reflect the transition from the open to the closed state, were estimated from measurements of current decay at potentials from −120 to −40 mV after briefly activating the channels (at −20 mV for 0.5 ms). As shown in Fig. 2F, the rates of current decay of Q10R mutant channels were significantly slower (P < 0.05) than those of WT channels across all deactivation potentials tested. While inactivation could make a substantive contribution to the kinetics of current decay in the −70 to −40 mV voltage range, current decay was slower over the entire voltage range studied, suggesting that like other IEM mutations, the Q10R mutation produces a significantly slower deactivation of sodium channels.

Steady-state fast-inactivation was achieved with a series of 500-ms prepulses (−150 to 0 mV in 10 mV increments) and the remaining non-inactivated channels were activated by a 40 ms step depolarization to −10 mV. When fitted with Boltzmann plots, the midpoint of fast-inactivation was not significantly different for WT (−81.6 ± 0.8 mV, n = 22) and Q10R (−82.6 ± 0.6 mV, n = 21) channels (Fig. 3A).

Steady-state slow-inactivation was determined with 30 s prepulses ranging from −130 to 10 mV followed by a 100 ms hyperpolarization at −120 mV to remove fast inactivation. Remaining available channels were activated by a 20 ms test pulse to −10 mV. The Q10R mutation enhanced steady-state slow-inactivation and shifted the midpoint by −4.8 mV (P < 0.01) from −59.5 ± 1.0 mV (n = 18) for WT to −64.3 ± 1.0 mV (n = 15) for Q10R (Fig. 3B). The offset for the slow-inactivation of Q10R mutant channels (18 ± 1%, n = 15; P < 0.01) was significantly reduced, compared to that of WT channels (22 ± 1%, n = 18).

Recovery from fast-inactivation, investigated using pairs of pulses with an incrementally increasing recovery time at four different recovery potentials (−100, −90, −80 and −70 mV), was fitted with an exponential function. Q10R mutation did not change the repriming kinetics at any of these four potentials (data not shown). The development of closed-state inactivation was similar for WT and Q10R mutant channels at the three different potentials tested (−80, −70 and −60 mV) (data not shown). Ramp currents, elicited with slow depolarizations from −100 to 20 mV over 600 ms, did not display different normalized amplitudes for Q10R channels (0.26 ± 0.02%, n = 15) and WT channels (0.27 ± 0.03%, n = 15).

Splice variant switching does not enhance Na$_v$1.7/Q10R gain-of-function

Four Na$_v$1.7 splicing isoforms have been detected within DRG neurons (Raymond *et al*., 2004), carrying variants of exon 5

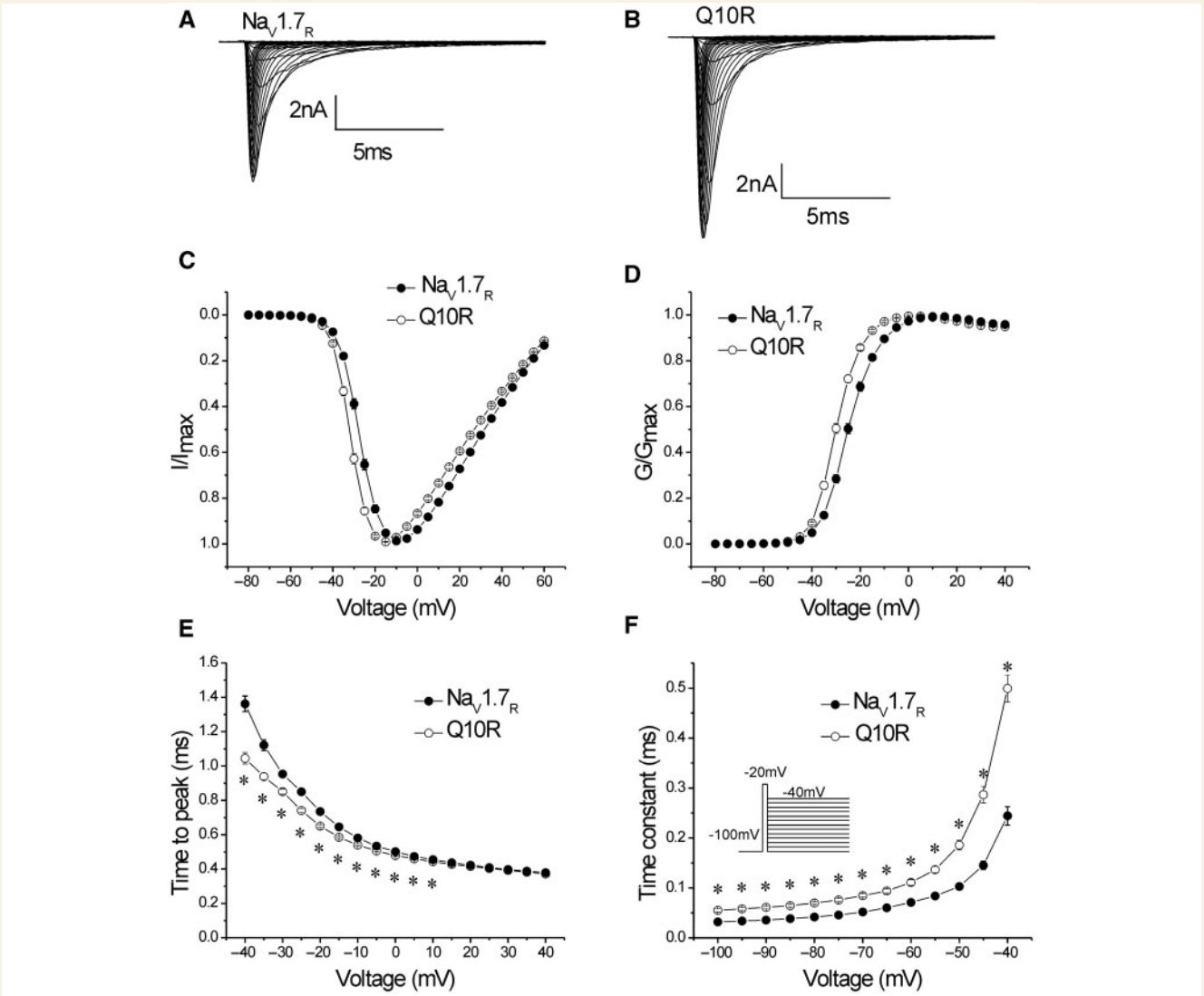

Figure 2 The Q10R mutation alters voltage-dependent activation of $Na_v1.7$ channels. Representative currents produced by cells expressing WT (**A**) or mutant Q10R channels (**B**), elicited using a range of depolarizations (−80 to 60 mV) from a holding potential of −100 mV. (**C**) Normalized *I–V* curves for $Na_v1.7_R$ ($n = 43$) and Q10R mutant ($n = 48$) channels. (**D**) Comparison of voltage-dependent activation of $Na_v1.7_R$ and Q10R mutant channels. A hyperpolarizing shift (−5.3 mV) of activation was observed in Q10R mutant channels. (**E**) As a measure of activation kinetics, time-to-peak is shown for step depolarizations, with the mutation Q10R opening faster than $Na_v1.7_R$ at potentials ranging from −40 to 10 mV, $^*P < 0.05$, Q10R versus WT. (**F**) Q10R ($n = 19$) deactivates significantly slower than $Na_v1.7_R$ ($n = 13$). Cells were held at −100 mV and tail currents were generated by a brief 0.5 ms depolarization to −20 mV followed by a series of repolarizations ranging from −100 to −40 mV, $^*P < 0.05$, Q10R versus WT.

that have been termed 'neonatal' (N) and 'adult' (A), and loop 1 variants that have been termed 'short' (S) and 'long' (L). To determine whether a switch in splice variant expression might result in a larger effect of the Q10R mutation, we expressed transiently the mutation in the adult-long (AL) form of $hNa_v1.7$ and used whole-cell patch-clamp recording to measure the effects of the mutation.

Figure 4A and B shows representative sodium currents recorded from cells expressing the WT $Na_v1.7_R$/AL channel and cells expressing the Q10R/AL mutants. The peak current densities of the two constructs were: WT/AL channel (343 ± 46 pA/pF; $n = 29$), and Q10R/AL channel (593 ± 54 pA/pF; $n = 30$). Similar to the NS version of $Na_v1.7$, the midpoint of activation of Q10R/AL (Fig. 4C, D) was significantly shifted by −5.1 mV in a hyperpolarizing direction (−27.8 ± 0.7 mV, $n = 30$; $P < 0.001$) compared to WT/AL channels (−22.7 ± 0.6 mV, $n = 29$).

The rate of activation for Q10R/AL channels was significantly faster ($P < 0.05$) than WT/AL at potentials ranging from −40 to 40 mV (Fig. 4E), but the shift was not larger than in the NS background. Similarly, the Q10R/AL mutant channels are characterized by a significantly slower deactivation of sodium currents compared to WT/AL (Fig. 4F), but the shift in the rate of current decay was not different from that in the NS background.

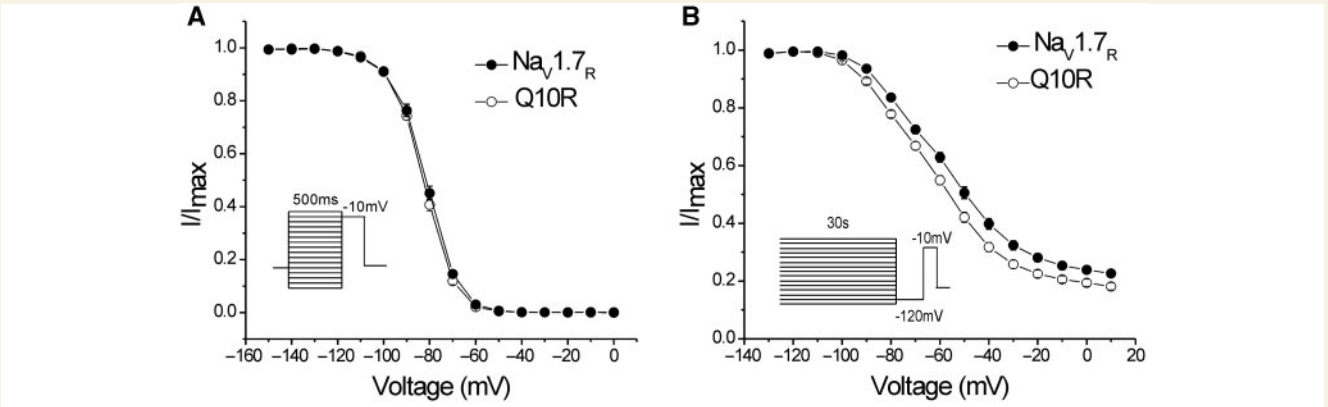

Figure 3 The Q10R mutation does not alter steady-state fast inactivation, but alters steady-state slow inactivation of $Na_V1.7$ channels. (**A**) Steady-state fast inactivation was examined using a series of 500 ms prepulses from −150 to 0 mV followed by 40 ms test pulses at −10 mV. The midpoints of fast-inactivation for $Na_V1.7_R$ channels ($n = 22$) and Q10R mutant channels ($n = 21$) were similar. (**B**) Steady-state slow-inactivation was assessed using a 20 ms pulse to −10 mV after a 30 s prepulse to potentials ranging from −130 to 10 mV followed by a 100 ms pulse to −120 mV to remove fast inactivation. The mutation Q10R ($n = 15$) shifts steady-state slow inactivation of $Na_V1.7_R$ ($n = 18$) by −4.8 mV.

As in the NS background, the midpoint of fast-inactivation was not different for WT/AL (−82.1 ± 0.9 mV, $n = 16$) and Q10R/AL (−82.7 ± 1.2 mV, $n = 15$) channels (Fig. 5A). Q10R/AL displayed enhanced steady-state slow-inactivation and significantly shifted the midpoint by −5.3 mV ($P < 0.01$) from −61.0 ± 1.1 mV ($n = 11$) for WT/AL to −66.3 ± 1.1 mV ($n = 9$) for Q10R/AL (Fig. 5B), a shift that was similar to the shift in the NS background. The offset for the slow-inactivation of the Q10R/AL mutant channels (12 ± 1%, $n = 9$) was significantly reduced ($P < 0.05$) compared to that of WT/AL (16 ± 2%, $n = 11$).

Recovery from inactivation in the AL background showed similar rates at −100, −90, −80 and −70 mV, as in the NS background (data not shown). The development of closed-state inactivation was also similar between WT/AL and Q10R/AL mutant channels (data not shown). The normalized amplitudes of ramp currents, elicited with slow depolarizations from −100 to 20 mV over 600 ms, were not different for Q10R/AL channels (0.22 ± 0.04%, $n = 10$) and WT/AL channels (0.24 ± 0.03%, $n = 10$), similar to the NS background.

Taken together, these results show that the effects of the Q10R mutation are not larger in the AL, compared to those seen in the NS splicing isoform of $Na_V1.7$.

Current-clamp recording: Q10R makes DRG neurons hyperexcitable, but to a smaller degree than early-onset erythromelalgia mutation I848T

To assess the effect of the Q10R mutation on excitability, we expressed WT and Q10R channels in small (<25 μm) DRG neurons and performed current-clamp recordings. Because the shift in activation and ramp response produced by Q10R is smaller than those produced by early-onset IEM mutations, we predicted that Q10R would produce DRG neuron hyperexcitability, but to a lesser degree than that produced by early-onset IEM mutations. To test this hypothesis, we studied the I848T IEM mutation, linked to a sporadic case with early-onset of clinical symptoms at the age of 5 years old (Yang *et al*., 2004), which has been shown to produce a 13.8 mV hyperpolarizing shift in activation (Cummins *et al*., 2004).

The resting membrane potential (−63.4 ± 0.8 mV, $n = 46$) of DRG neurons expressing WT channels was similar to that of DRG neurons expressing Q10R (−62.2 ± 1.2 mV, $n = 33$), whereas I848T mutant channels depolarized resting membrane potential of DRG neurons by 4.4 mV (−59.0 ± 1.9 mV, $n = 27$; $P < 0.05$, one way ANOVA followed by Tukey *post hoc* test). Early studies have shown that the membrane depolarization produced by some IEM mutations is only a partial contributor to increased DRG neuron excitability, with other factors such as the shift in $Na_V1.7$ activation and slower deactivation also contributing (Harty *et al*., 2006; Sheets *et al*., 2007). Moreover, previous studies have shown that IEM mutations produce hyperexcitability in DRG neurons at resting potentials close to −60 mV, where tetrodotoxin-sensitive sodium channels (including $Na_V1.7$) are partially inactivated, due to the presence of $Na_V1.8$ channels (which are relatively resistant to inactivation by depolarization) in these cells (Rush *et al*., 2006). Consistent with this schema, though Q10R mutant channels have no effects on the resting membrane potential, expression of Q10R channels significantly decreased the current threshold for action potential firing. Transfection with I848T mutant channels also resulted in a significantly lower current threshold for action potential firing. Fig. 6A shows traces from a representative DRG neuron expressing WT channels. Although the cell responded to 180 pA sub-threshold current injections with small, graded membrane potential depolarizations, all-or-none action potentials required stimuli of 190 pA (current threshold for this neuron). Figure 6B shows traces from a representative DRG neuron expressing Q10R channels. For this neuron, a lower 130 pA threshold current injection could produce an overshooting action potential, and further

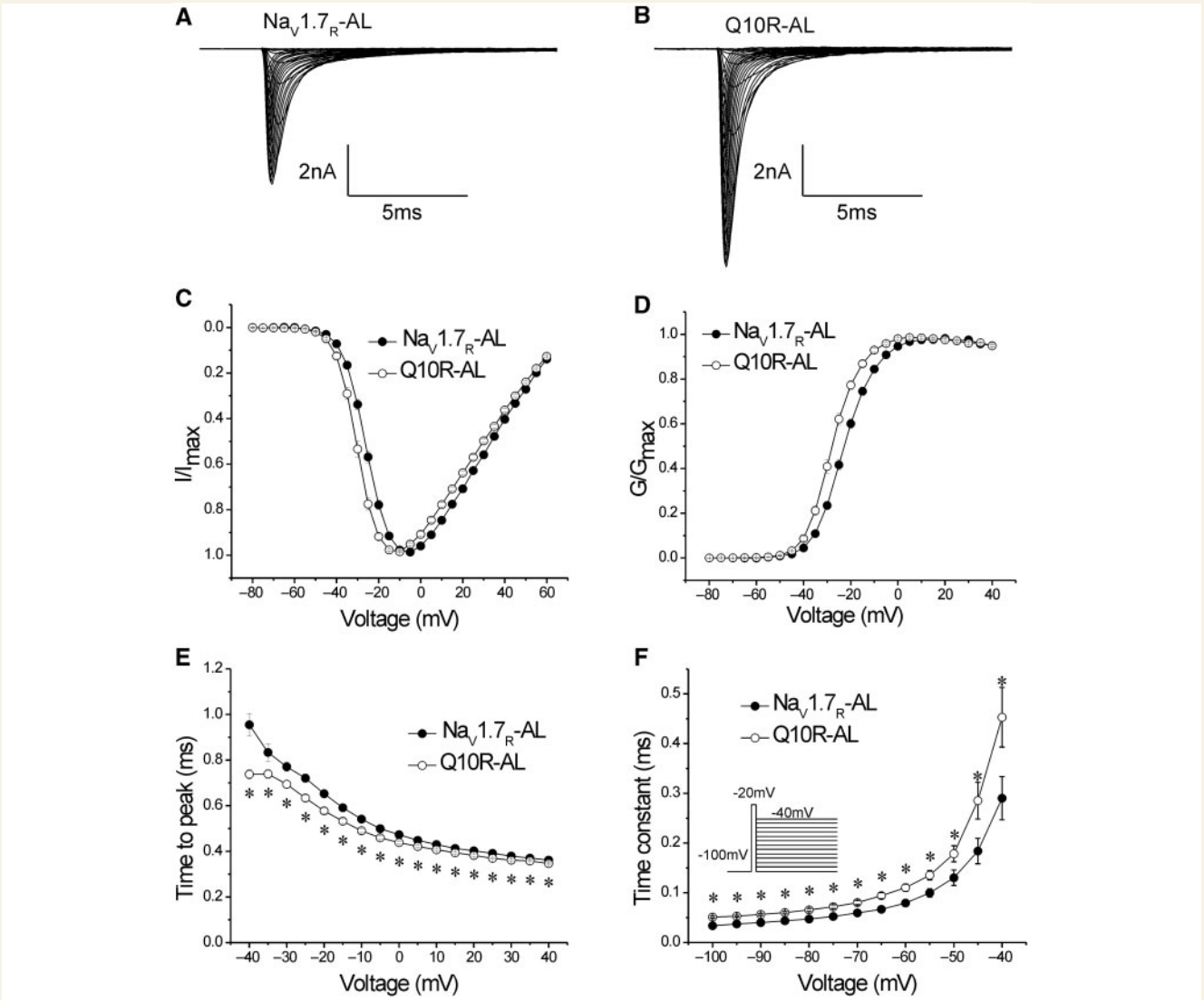

Figure 4 The Q10R mutation within the AL background does not introduce a larger alteration in the voltage-dependent activation of $Na_V1.7$ channels. Representative currents produced by cells expressing the $Na_V1.7_R$/AL variant of the WT (**A**) or the mutant Q10R/AL channels (**B**), elicited using a range of depolarizations (−80 to 60 mV) from a holding potential of −100 mV. (**C**) Normalized *I–V* curves for $Na_V1.7_R$/AL ($n = 29$) and Q10R/AL mutant ($n = 30$) channels. (**D**) Comparison of voltage-dependent activation of $Na_V1.7_R$/AL and Q10R/AL mutant channels. A hyperpolarizing shift (−5.1 mV) of activation was observed in Q10R/AL mutant channels. (**E**) Activation kinetics, time to peak is shown for step depolarizations, with the mutation Q10R/AL opening faster than $Na_V1.7_R$/AL at potentials ranging from −40 to 40 mV. $^*P < 0.05$. (**F**) Q10R/AL ($n = 10$) deactivates significantly slower than $Na_V1.7_R$/AL ($n = 10$). Cells were held at −100 mV and tail currents were generated by a brief 0.5 ms depolarization to −20 mV followed by a series of repolarizations ranging from −100 to −40 mV. $^*P < 0.05$.

increased current injection resulted in all-or-none action potentials of similar amplitude. Typical traces from a DRG neuron expressing I848T mutant channels are shown in Fig. 6C, where 90 pA current injections could produce an action potential. As illustrated in Fig. 6D, current threshold was significantly reduced ($P < 0.05$, Kruskal–Wallis test followed by Dunn procedure) for DRG neurons expressing Q10R (122 ± 13 pA, $n = 33$) and I848T (92 ± 14 pA, $n = 27$), compared with WT (188 ± 13 pA, $n = 46$); neurons expressing I848T showed a trend towards a threshold that was lower than for neurons expressing Q10R, but this was not statistically significant.

As reported by Renganathan *et al*. (2001), ~50% of native small DRG neurons fire repetitively in response to prolonged suprathreshold current stimuli. In the present study, 54% (25 out of 46) of DRG neurons expressing WT channels fired repetitively in response to suprathreshold current injections. A slightly higher percentage, 64% (21 out of 33), of DRG neurons expressing Q10R mutant channels fired, repetitively. In contrast, 93% (25 out of 27) of DRG neurons expressing I848T mutant channels fired repetitively.

The frequency of firing across a broad range of current injections (25–500 pA) tended to be different for DRG neurons

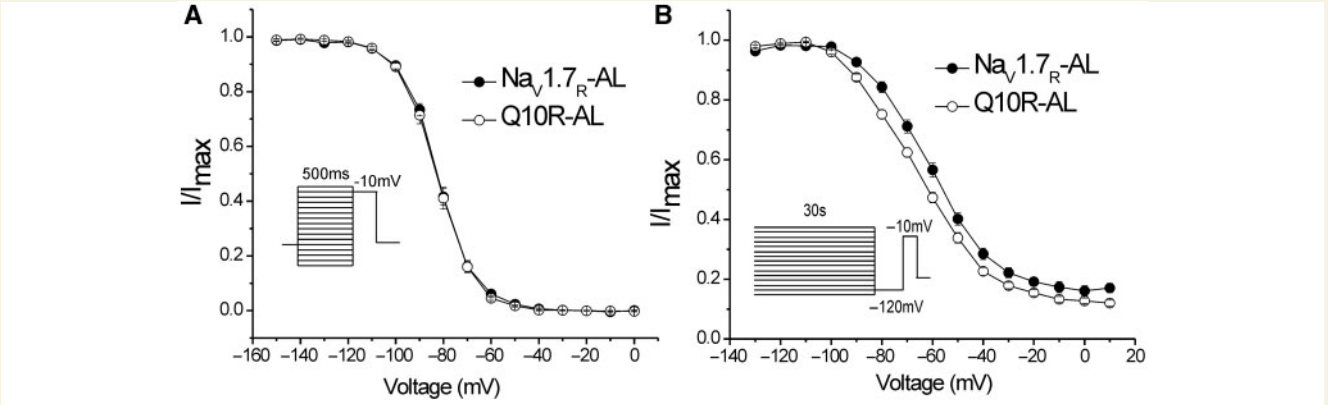

Figure 5 The Q10R/AL mutation does not alter steady-state fast-inactivation, but alters steady-state slow-inactivation of $Na_v1.7$ channels. (**A**) Steady-state fast-inactivation was examined using a series of 500 ms prepulses from −150 to 0 mV followed by 40 ms test pulses at −10 mV. The midpoints of fast-inactivation for $Na_v1.7_R$/AL channels ($n = 16$) and Q10R/AL mutant channels ($n = 15$) were similar. (**B**) Steady-state slow-inactivation was assessed using a 20 ms pulse to −10 mV after a 30 s prepulse to potentials ranging from −130 to 10 mV followed by a 100 ms pulse to −120 mV to remove fast inactivation. The mutation Q10R/AL ($n = 9$) shifts steady-state slow-inactivation of $Na_v1.7_R$/AL ($n = 11$) by −5.2 mV.

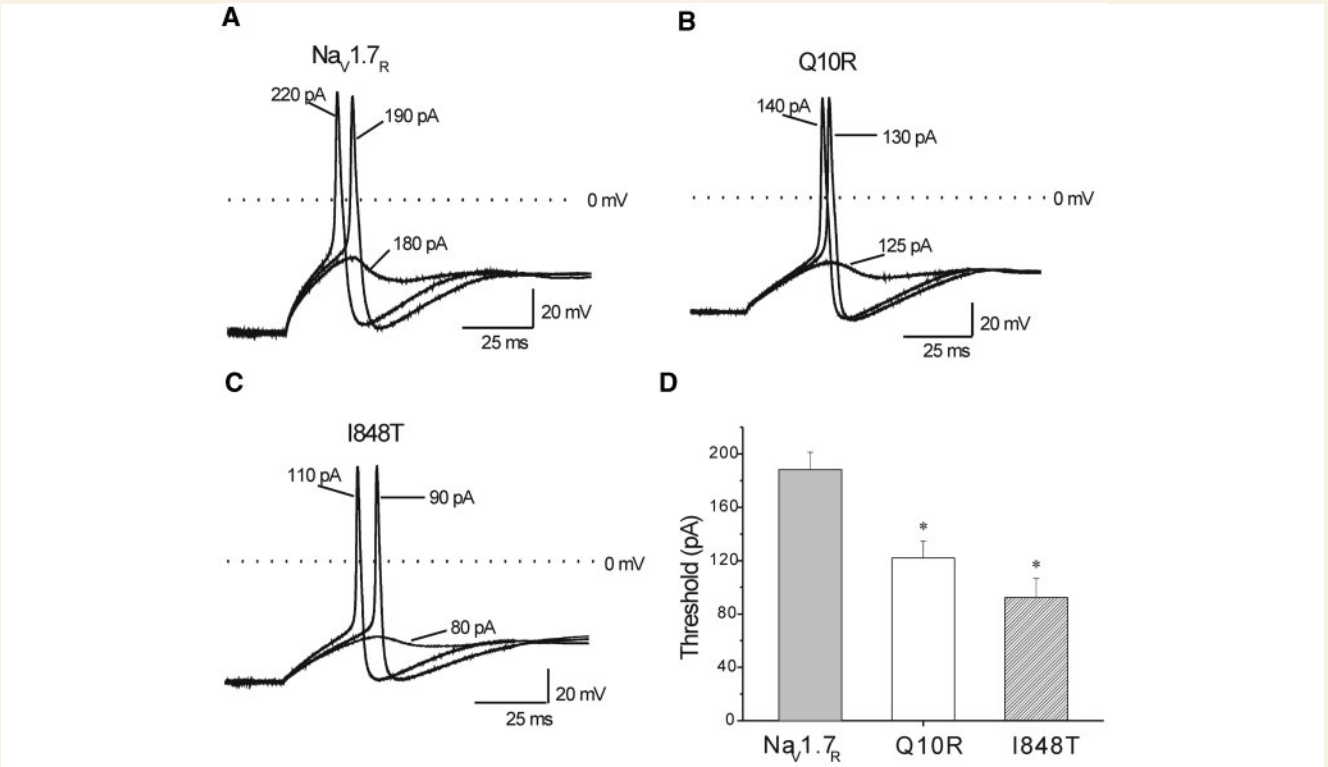

Figure 6 Both Q10R and I848T mutations decrease action potential threshold in small DRG neurons. (**A**) Representative traces from a cell expressing $Na_v1.7$ WT channels, showing subthreshold response to 180 pA current injection and subsequent action potentials evoked by injections of 190 pA (current threshold for this neuron) and 220 pA. (**B**) Representative traces from a cell expressing Q10R channels, showing a lower current threshold (130 pA for this cell) for action potential generation. (**C**) Representative traces from a DRG neuron expressing I848T channels, showing a significantly lower current threshold (90 pA for this cell) for action potential generation. (**D**) Compared with cells expressing $Na_v1.7$ WT channels ($n = 46$), current threshold for action potential generation decrease significantly in those expressing Q10R channels ($n = 33$) and I848T channels ($n = 27$). $^*P < 0.05$.

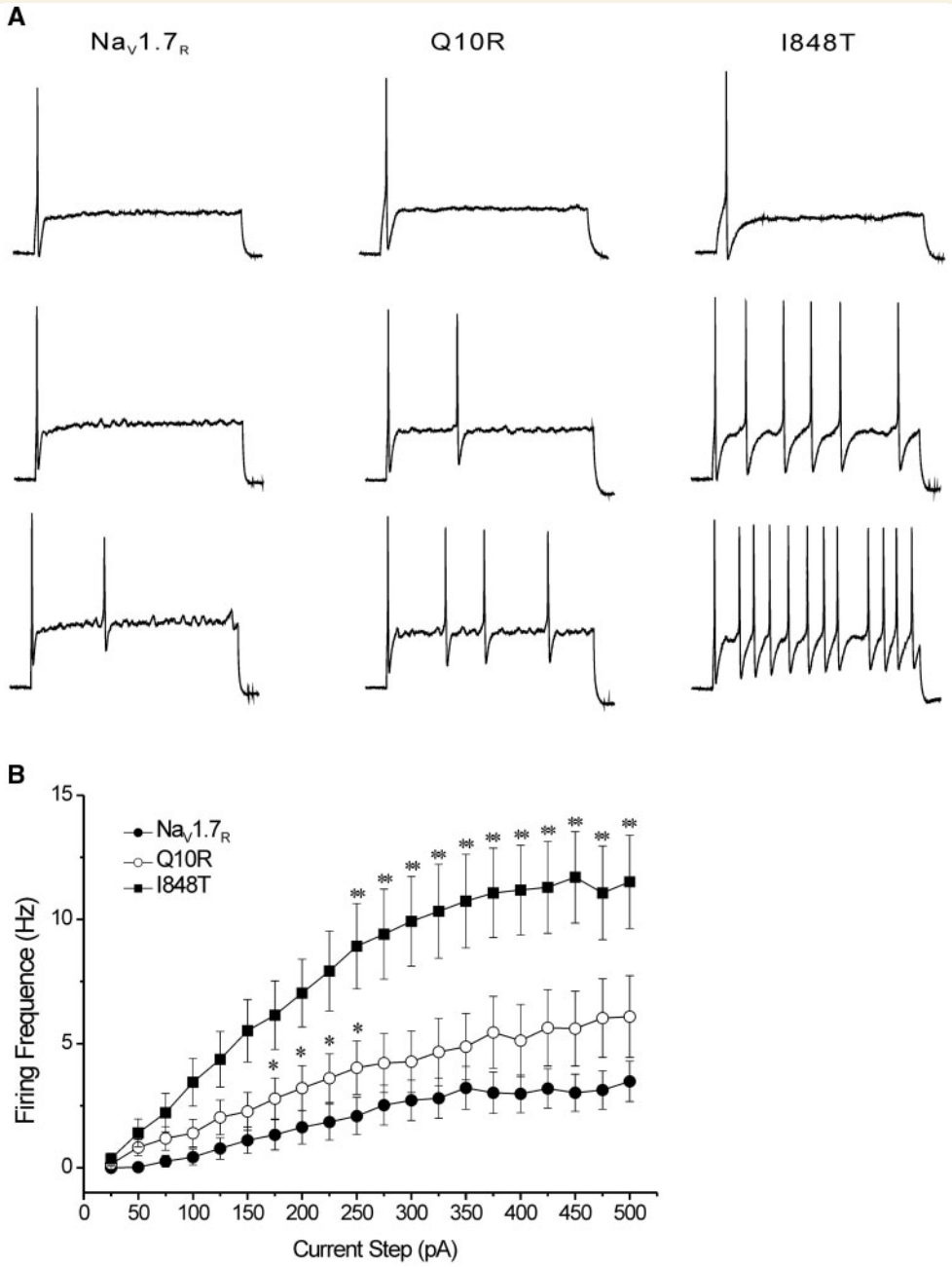

Figure 7 Q10R and I848T mutations increase firing frequency in small DRG neuron, but to different degrees. (**A**) Response of cells expressing WT, Q10R and I848T channels, respectively, to 1 s depolarizing current steps that are 1X, 2X and 3X (top, middle and bottom traces, respectively) the current threshold for action potential generation. (**B**) Comparison of mean fire frequency among cells expressing WT, Q10R and I848T channels across the range of current injections from 25 to 500 pA. $*P<0.05$, Q10R versus WT; $**P<0.05$, I848T versus Q10R.

transfected with WT versus Q10R versus I848T channels. The responses of three representative cells which expressed WT, Q10R or I848T channels, respectively, to 1 s depolarizing current steps at 1X, 2X and 3X current threshold are shown in Fig. 7A. Cells expressing WT channels ($n=46$) usually generate only one or two spikes in response to current injections at 2X or 3X the current threshold, while cells expressing Q10R ($n=33$) and I848T ($n=27$) mutant channels displayed firing frequencies higher than those of cells expressing WT channels. Figure 7B shows the firing frequencies of cells expressing WT, Q10R and I848T channels and illustrates the trend of cells expressing I848T to fire at higher frequencies than cells expressing Q10R which, in turn, fired at higher frequencies than cells expressing WT channels. Our analysis has also shown no evidence that after-hyperpolarizations were significantly different in DRG neurons expressing WT or mutant channels.

Discussion

IEM, an autosomal dominant disorder in which patients experience severe burning pain in the distal extremities in response to mild warmth or exercise, has been directly linked to gain-of-function mutations of sodium channel $Na_v1.7$. Almost all physiologically-characterized cases of IEM have been associated with onset at young ages, usually before the age of 6 years (Dib-Hajj *et al*., 2007; Drenth and Waxman, 2007). Only one family with later onset, with pain appearing first in the feet at ages ranging from 9 to 22 years, with onset at ages >17 years in five of seven family members and relatively slow progression (8 to 10 years) to involvement of the hands (Lee *et al*., 2007) has been characterized using voltage-clamp recordings (Cheng *et al*., 2008). Cheng *et al*. (2008) showed that the $Na_v1.7$ mutation in this second decade onset family, I136V, hyperpolarizes the voltage-dependence of activation of the channel, but to a smaller degree (−5.7 mV) than for the early-onset erythromelalgia mutations that have been studied to date (−7.6 to −13.8 mV). Here we report a new $Na_v1.7$ mutation, Q10R, in a patient with clinical onset of erythromelalgia at 14 years of age. We show that the Q10R mutation hyperpolarizes activation of the channel by only −5.3 mV, and does not produce a significant increase in the ramp response. Using current-clamp to study the effect of the Q10R mutation on DRG neuron firing and to compare its effect with that of I848T, an early-onset erythromelalgia mutation which shifts activation voltage-dependence more dramatically, we show that expression of Q10R induces hyperexcitability in these cells, but produces an increase in excitability that is smaller than the change produced by an early-onset erythromelalgia mutation I848T.

The Q10R mutation substitutes glutamine by arginine within the N-terminus of the $Na_v1.7$ channel, in contrast to most other $Na_v1.7$ erythromelalgia mutations studied to date, which have been localized to the S4 voltage sensor, the linker joining segments S4 and S5, or pore-lining segments S5 and S6 within domains I and II of the channel (Dib-Hajj *et al*., 2007). However, similar to Q10R, the I136V mutation (Lee *et al*., 2007), which is located within DI-S1, substitutes a residue within a part of the channel which has not been shown to have a substantial effect on channel kinetics or gating. Both of these mutations (Q10R and I136V) display a smaller shift in $V_{1/2}$ of activation, compared to the other IEM mutations, share a later onset of symptoms and are clinically characterized by delayed involvement of the hands. While the number of cases of late-onset IEM is small, this observation may point to a genotype–phenotype relationship, with mutations causing smaller effects on channel activation being associated with later onset, and less severity, of pain.

While a role of the N-terminus in regulating surface expression of a sodium channel isoform has been established for the sensory neuron-specific channel $Na_v1.8$ (Okuse *et al*., 2002), the role of the N-terminus in channel gating is only now becoming understood. Several mutations within the N-terminus of $Na_v1.1$ and $Na_v1.5$ have been linked to epilepsy (Lossin, 2009) and cardiac disorders (Tester *et al*., 2005), respectively, but the functional effects of these mutations on these channels have not been investigated in expression systems. A missense mutation in the N-terminus of $Na_v1.2$ associated with epilepsy has been found to slow inactivation, a change that may prolong residence of the mutant channel in the open state so as to produce neuronal hyperexcitability (Sugawara *et al*., 2001). The I141V mutation in $Na_v1.4$ associated with myotonia shifts the activation voltage-dependence −12.9 mV in a hyperpolarization direction, thereby increasing window current (Petitprez *et al*., 2008). Recently, it has been shown that substituting the N-terminus and transmembrane segments 1–3 of $Na_v1.2$ for those of $Na_v1.6$ conferred activation properties of $Na_v1.2$ on the chimera channel (Lee and Goldin, 2008). Since the chimera carried transmembrane segments in addition to the N-terminus, however, it is not possible to attribute the effect on activation to a particular sequence. Thus, the present study adds to the evidence for a specific role of the N-terminus of sodium channels in regulating activation properties of a sodium channel.

Because the hyperpolarizing shift in activation produced by Q10R is smaller than those produced by early-onset erythromelalgia mutations and Q10R did not enhance the ramp response, we predicted that Q10R would produce DRG neuron hyperexcitablility, but to a smaller degree than the early-onset mutations. Our current-clamp observations indicate that is indeed the case. The available data comparing this mutation, another IEM mutation linked to onset of pain in the second decade (Cheng *et al*., 2008) and mutations linked to early-onset pain thus suggest that there may be a correlation between the magnitude of the shift in voltage-dependence of activation, and the degree of hyperexcitability produced by the mutation. The only other second decade onset erythromelalgia mutation that has been studied shows a relatively small hyperpolarizing shift in activation (−5.7 mV) but increased ramp currents by 3-fold (Cheng *et al*., 2008). Supporting a relationship between the size of the activation shift and degree of hyperexcitability, computer simulations of the effect of $Na_v1.7$ mutant channels in DRG neurons demonstrate that the hyperpolarizing shift in channel activation plays a dominant role in producing neuronal hyperexcitability (Sheets *et al*., 2007).

$Na_v1.7$ is known to be present in four isoforms within DRG neurons, including isoforms that carry variants of exon 5 that have been termed 'neonatal' and 'adult', and of loop 1 which have been termed 'short' and 'long' (Raymond *et al*., 2004). Although the temporal sequence (if any) of a switch from the neonatal to the adult isoforms in humans is not known, we compared the effects of the Q10R mutation on neonatal and adult isoforms of $hNa_v1.7$, to examine the possibility that the mutation has a larger effect on the adult isoform. Our results do not support this hypothesis. Notably, the hyperpolarizing shift in activation produced by the mutation was slightly smaller (−5.1 mV) in the adult background than the shift in the neonatal background (−5.3 mV). Although it is not clear whether this shift is due to difference in the voltage-dependence of activation in the adult versus neonatal background, it should be noted that a study that compared splice variants of $Na_v1.7$ within a transient expression system (Chatelier *et al*., 2008) did not observe a difference in activation. These results suggest that the absence of symptoms in the first decade can not be explained by the predominance of

a neonatal $Na_v1.7$ splicing isoform, e.g. $Na_v1.7$/NS, because the Q10R/NS and Q10R/AL show a similar enhancement of channel activation compared to WT isoforms. Thus, our results do not provide evidence that adult onset of pain is due to a preferential effect of the mutation within the adult splice variant of $Na_v1.7$.

The sequence of events starting with $Na_v1.7$ mutations and resulting in pain with variable age of onset of symptoms in IEM patients is complex and, for some mutations, might depend upon molecular modifiers of the channel. Previous studies have shown that the effect of a given mutation can be influenced by a variant allele of a modifier locus. For example, the severity of $Na_v1.2$-related epilepsy is regulated by mutations in the potassium channel $K_v7.2$ (Kearney *et al*., 2006). However, the modifier locus does not have to carry a mutation, since the co-expression of the target and modifier genes within the same cell can yield a different outcome than expression of the target gene alone. Neurons co-expressing IEM mutant L858H $Na_v1.7$ channels together with $Na_v1.8$ become hyperexcitable, while neurons that lack $Na_v1.8$ become hypoexcitable (Rush *et al*., 2006). Thus, it is possible that the age of onset of IEM for some $Na_v1.7$ mutations may be linked to co-expression with different modifier genes.

Alternatively, the present results suggest that variable age of onset of IEM symptoms may depend on intrinsic properties of mutant $Na_v1.7$ channels. Age of onset of spinocerebellar ataxia type 6 (SCA6) is inversely proportional to the length of the CAG repeats of $Ca_v2.1$ (SCA6) (Zoghbi and Orr, 2000; Michalik and Van Broeckhoven, 2003). In this instance, pathogenesis is related to the age-dependent accumulation of the mutant $Ca_v2.1$ protein rather than changes in the current density or gating properties of the channel (Watase *et al*., 2008). In contrast, the mutant $Na_v1.7$ channel that we report here in a patient with late-onset IEM displays different biophysical properties and effects on DRG neuron hyperexcitability compared to $Na_v1.7$ mutations in patients with early-onset IEM (Dib-Hajj *et al*., 2007). By linking the magnitude of these changes in function at the ion channel and DRG neuron levels to age of pain onset, we propose a genotype–phenotype correlation at the clinical, cellular and molecular levels within IEM which may explain the early- versus late-onset of symptoms.

Acknowledgements

We thank Dr Xiaoyang Cheng and Dr Mark Estacion for helpful discussions, and Larry Macala and Bart Toftness for technical assistance.

Funding

Rehabilitation Research Service and Medical Research, Department of Veterans Affairs (to S.G.W.); National Multiple Sclerosis Society (to S.G.W.); Erythromelagia Association (to S.G.W.); Program for New Century Excellent Talents in University (NCET-06-0015 to Y.Y.); Fok Ying Tong Education Foundation (111039 to Y.Y.).

References

Black JA, Dib-Hajj S, McNabola K, Jeste S, Rizzo MA, Kocsis JD, et al. Spinal sensory neurons express multiple sodium channel alpha-subunit mRNAs. Mol Brain Res 1996; 43: 117–31.

Chatelier A, Dahllund L, Eriksson A, Krupp J, Chahine M. Biophysical properties of human Nav1.7 splice variants and their regulation by protein kinase A. J Neurophysiol 2008; 99: 2241–50.

Cheng X, Dib-Hajj SD, Tyrrell L, Waxman SG. Mutation I136V alters electrophysiological properties of the Nav1.7 channel in a family with onset of erythromelalgia in the second decade. Mol Pain 2008; 4: 1.

Choi JS, Dib-Hajj SD, Waxman SG. Inherited erythermalgia. Limb pain from an S4 charge-neutral Na channelopathy. Neurology 2006; 67: 1563–7.

Cummins TR, Dib-Hajj SD, Black JA, Akopian AN, Wood JN, Waxman SG. A novel persistent tetrodotoxin-resistant sodium current in SNS-null and wild-type small primary sensory neurons. J Neurosci 1999; 19: RC43.

Cummins TR, Dib-Hajj SD, Waxman SG. Electrophysiological properties of mutant Nav1.7 sodium channels in a painful inherited neuropathy. J Neurosci 2004; 24: 8232–6.

Cummins TR, Howe JR, Waxman SG. Slow closed-state inactivation: a novel mechanism underlying ramp currents in cells expressing the hNE/PN1 sodium channel. J Neurosci 1998; 18: 9607–19.

Dib-Hajj SD, Cummins TR, Black JA, Waxman SG. From genes to pain: $Na_v1.7$ and human pain disorders. Trends Neurosci 2007; 30: 555–63.

Dib-Hajj SD, Estacion M, Jarecki BW, Tyrrell L, Fischer TZ, Lawden M, et al. Paroxysmal extreme pain disorder M1627K mutation in human Nav1.7 renders DRG neurons hyperexcitable. Mol Pain 2008; 4: 37.

Dib-Hajj SD, Rush AM, Cummins TR, Hisama FM, Novella S, Tyrrell L, et al. Gain-of-function mutation in Nav1.7 in familial erythromelalgia induces bursting of sensory neurons. Brain 2005; 128: 1847–54.

Djouhri L, Newton R, Levinson SR, Berry CM, Carruthers B, Lawson SN. Sensory and electrophysiological properties of guinea-pig sensory neurones expressing $Na_v1.7$ (PN1) Na^+ channel alpha-subunit protein. J Physiol (Lond) 2003; 546: 565–76.

Drenth JP, Waxman SG. Mutations in sodium-channel gene SCN9A cause a spectrum of human genetic pain disorders. J Clin Invest 2007; 117: 3603–9.

Han C, Rush AM, Dib-Hajj SD, Li S, Xu Z, Wang Y, et al. Sporadic onset of erythermalgia: a gain-of-function mutation in Nav1.7. Ann Neurol 2006; 59: 553–8.

Harty TP, Dib-Hajj SD, Tyrrell L, Blackman R, Hisama FM, Rose JB, et al. $Na_V1.7$ mutant A863P in erythromelalgia: effects of altered activation and steady-state inactivation on excitability of nociceptive dorsal root ganglion neurons. J Neurosci 2006; 26: 12566–75.

Herzog RI, Cummins TR, Ghassemi F, Dib-Hajj SD, Waxman SG. Distinct repriming and closed-state inactivation kinetics of Nav1.6 and Nav1.7 sodium channels in mouse spinal sensory neurons. J Physiol (Lond) 2003; 551: 741–50.

Kearney JA, Yang Y, Beyer B, Bergren SK, Claes L, Dejonghe P, et al. Severe epilepsy resulting from genetic interaction between Scn2a and Kcnq2. Hum Mol Genet 2006; 15: 1043–8.

Klugbauer N, Lacinova L, Flockerzi V, Hofmann F. Structure and functional expression of a new member of the tetrodotoxin-sensitive voltage-activated sodium channel family from human neuroendocrine cells. EMBO J 1995; 14: 1084–90.

Lampert A, Dib-Hajj SD, Tyrrell L, Waxman SG. Size matters: Erythromelalgia mutation S241T in Nav1.7 alters channel gating. J Biol Chem 2006; 281: 36029–35.

Lee A, Goldin AL. Role of the amino and carboxy termini in isoform-specific sodium channel variation. J Physiol 2008; 586: 3917–26.

Lee MJ, Yu HS, Hsieh ST, Stephenson DA, Lu CJ, Yang CC. Characterization of a familial case with primary erythromelalgia from Taiwan. J Neurol 2007; 254: 210–4.

Lossin C. A catalog of SCN1A variants. Brain Dev 2009; 31: 114–30.

Michalik A, Van Broeckhoven C. Pathogenesis of polyglutamine disorders: aggregation revisited. Hum Mol Genet 2003; 12: R173–86.

Okuse K, Malik-Hall M, Baker MD, Poon WY, Kong H, Chao MV, et al. Annexin II light chain regulates sensory neuron-specific sodium channel expression. Nature 2002; 417: 653–6.

Petitprez S, Tiab L, Chen L, Kappeler L, Rösler KM, Schorderet D, et al. A novel dominant mutation of the Nav1.4 alpha-subunit domain I leading to sodium channel myotonia. Neurology 2008; 71: 1669–75.

Raymond CK, Castle J, Garrett-Engele P, Armour CD, Kan Z, Tsinoremas N, et al. Expression of alternatively spliced sodium channel alpha-subunit genes: Unique splicing patterns are observed in dorsal root ganglia. J Biol Chem 2004; 279: 46234–41.

Renganathan M, Cummins TR, Waxman SG. Contribution of Nav1.8 sodium channels to action potential electrogenesis in DRG neurons. J Neurophysiol 2001; 86: 629–40.

Rizzo MA, Kocsis JD, Waxman SG. Slow sodium conductances of dorsal root ganglion neurons: intraneuronal homogeneity and interneuronal heterogeneity. J Neurophysiol 1994; 72: 2796–815.

Rush AM, Dib-Hajj SD, Liu S, Cummins TR, Black JA, Waxman SG. A single sodium channel mutation produces hyper- or hypoexcitability in different types of neurons. Proc Natl Acad Sci USA 2006; 103: 8245–50.

Sangameswaran L, Fish LM, Koch BD, Rabert DK, Delgado SG, Ilnicka M, et al. A novel tetrodotoxin-sensitive, voltage-gated sodium channel expressed in rat and human dorsal root ganglia. J Biol Chem 1997; 272: 14805–9.

Sheets PL, Jackson Ii JO, Waxman SG, Dib-Hajj S, Cummins TR. A Nav1.7 channel mutation associated with hereditary erythromelalgia contributes to neuronal hyperexcitability and displays reduced lidocaine sensitivity. J Physiol (Lond) 2007; 581: 1019–31.

Sugawara T, Tsurubuchi Y, Agarwala KL, Ito M, Fukuma G, Mazaki-Miyazaki E, et al. A missense mutation of the Na+ channel alpha II subunit gene Na(v)1.2 in a patient with febrile and afebrile seizures causes channel dysfunction. Proc Natl Acad Sci USA 2001; 98: 6384–9.

Tester DJ, Will ML, Haglund CM, Ackerman MJ. Compendium of cardiac channel mutations in 541 consecutive unrelated patients referred for long QT syndrome genetic testing. Heart Rhythm 2005; 2: 507–17.

Toledo-Aral JJ, Moss BL, He ZJ, Koszowski AG, Whisenand T, Levinson SR, et al. Identification of PN1, a predominant voltage-dependent sodium channel expressed principally in peripheral neurons. Proc Natl Acad Sci USA 1997; 94: 1527–32.

Watase K, Barrett CF, Miyazaki T, Ishiguro T, Ishikawa K, Hu Y, et al. Spinocerebellar ataxia type 6 knockin mice develop a progressive neuronal dysfunction with age-dependent accumulation of mutant CaV2.1 channels. Proc Natl Acad Sci USA 2008; 105: 11987–92.

Waxman SG. A channel sets the gain on pain. Nature 2006; 444: 831–2.

Yang Y, Wang Y, Li S, Xu Z, Li H, Ma L, et al. Mutations in SCN9A, encoding a sodium channel alpha subunit, in patients with primary erythermalgia. J Med Genet 2004; 41: 171–4.

Zoghbi HY, Orr HT. Glutamine repeats and neurodegeneration. Annu Rev Neurosci 2000; 23: 217–47.